

A topological principle for photovoltaics: Shift current in intrinsically polar insulators

A. Alexandradinata¹

¹Physics Department, University of California Santa Cruz, Santa Cruz, CA 95064, USA
(Dated: April 11, 2022)

To realize an efficient solar cell without inhomogeneous doping, one would like to maximize the shift component of the bulk photovoltaic current, in noncentric semiconductors with wide band gaps. I achieve this maximization for a new class of topological insulators whose band topology is *only* compatible with a polar crystal class. For such insulators, it is impossible to continuously tune the \mathbf{k} -dependent electron-hole dipole moment (or ‘shift vector’) to zero throughout the Brillouin zone. Averaging the shift vector over all high-symmetry cross-sections of the Brillouin zone gives *exactly* a rational multiple of a Bravais lattice vector, which points parallel to the polar axis. Even with wide band gaps, the frequency-integrated shift conductivity of intrinsically polar insulators greatly exceeds e^3/h^2 , and is at least three orders of magnitude larger than the conductivity of the prototypical ferroelectric BaTiO₃, challenging a widely-held expectation that small band gaps are necessary for large shift currents in topological materials. Close to a topological phase transition, the integrated conductivity diverges as $|E_g|^{-1/2}$ with E_g the band gap, suggesting an application to ultrafast infrared detection.

CONTENTS

References

14

I. Motivation and results	1
II. Theory of intrinsically polar insulators	3
A. Berry-curvature invariant that breaks centrosymmetry	3
B. Optical vortices break centrosymmetry	4
C. Shift obstruction relation	4
D. Implications for the shift connection	6
III. Model Hamiltonians of intrinsically polar insulators	6
A. Model with second-class phase transition	6
1. Flatband limit with zero optical vorticity	6
2. Optical phase transition	7
3. Energetic phase transition	7
4. Figure of merit	8
B. Model with first-class phase transition	9
IV. Greater variety of intrinsically polar insulators	9
A. Beyond a monatomic basis	9
B. Beyond two-band, reflection-symmetric Hamiltonians	10
V. The tight-binding approximation of the shift current: justification and pitfalls	11
A. Nature of the approximation	11
B. Semi-empirical justification of the approximation	11
C. Rigorous justification of the approximation	11
D. The discrete-space approximation for two bands	11
VI. Discussion and outlook	12
A. Recapitulation and fresh motivation of results	12
B. Outlook for ab-initio-based material searches	13
1. Materials with nontrivial optical vorticity	13
2. Intrinsically polar materials	13
Acknowledgments	14

I. MOTIVATION AND RESULTS

The uniform illumination of a homogeneous but noncentric material generates a direct photocurrent.[1] Part of this photocurrent originates from the positional displacement (or ‘shift’) of quasiparticles as they vertically transit between bands.[2] A geometric theory of the ‘shift current’ has developed based on geometric interpretations of the electron polarization[3–5] and the dipole matrix element.[6] In particular, the shift vector has been related to a geometric Berry phase[2, 7–9] which may take any generic value – it is not symmetry-fixed to a rational multiple of 2π . The theory of the shift current is thus geometrical without being topological – lacking the defining quality of quantization that is robust to perturbations.¹

Why was no quantized geometric phase found in previous investigations[11–16] of the shift current in topological materials? Because it is possible to continuously deform the insulating tight-binding Hamiltonian (or semimetallic low-energy Hamiltonian) to be centrosymmetric with vanishing shift current, while remaining in the same topological phase. This implies for the studied classes of topological materials that nontrivial topology of the wave function is not, by itself, a sufficient condition for a nontrivial shift; further supplemental conditions must be added to ensure the shift, e.g., proximity to a topological phase transition,[16] or tilting[11–13] (and warping[15]) of energy dispersions.

Aiming to forgo all supplemental conditions, this work introduces a new class of topological insulators for which

¹ Topological invariants exist for the circular photogalvanic effect[10] and the photovoltaic Hall effect[6].

wave-function topology is a sufficient condition for a non-trivial shift. The introduced class contrasts from previous case studies in being *intrinsically polar*, meaning that the topological distinction between trivial and nontrivial insulators only exists in noncentric crystal classes[17] that are polar/pyroelectric. The sufficient condition reads as follows:

(P1) For intrinsically polar insulators, a geometric quantity exists that inputs band wave functions and outputs an integer; if this integer is nonzero, the \mathbf{k} -dependent shift vector cannot be continuously tuned to zero throughout the Brillouin zone.

The shift vector $\mathbf{R}_{mn}^{ab}(\mathbf{k})$ is the positional shift (in the a direction) of a wave packet (with average wavevector \mathbf{k}) that is vertically excited from band n to band m , as it absorbs a photon that is linearly polarized (in the b direction) with negligible momentum.[2] In terms of the Berry connection $A_{ll'} = \langle u_{l\mathbf{k}} | i\nabla_{\mathbf{k}} u_{l'\mathbf{k}} \rangle$,

$$\mathbf{R}_{mn}^{ab}(\mathbf{k}) = \partial_{k_a} \phi_{mn}^b + A_{mm}^a - A_{nn}^a, \quad A_{mn}^b = |A_{mn}^b| e^{-i\phi_{mn}^b}, \quad (1)$$

with $\langle u_{l\mathbf{k}} | u_{l'\mathbf{k}} \rangle = \delta_{ll'}$ being the normalization for the wave function within a primitive unit cell. ϕ_{mn}^b is the phase of the band-off-diagonal Berry connection, which enters the theory through the dipole matrix element $eE^b A_{mn}^b$. The geometric quantity alluded to in Proposition (P1) is expressed in Eq. (7) in terms of a quantized Berry-Zak phase and the net vorticity of the dipole matrix element.

In evocative terms, the topological knot of the electronic wave function carries an unremovable polarity; in precise terms:

(P2) For an intrinsically polar insulator with a reflection symmetry, averaging the shift vector over either reflection-invariant \mathbf{k} -plane gives *exactly* a Bravais lattice vector.

There being two such \mathbf{k} -plane gives two independent vectors: $\vec{R}(0)$ and $\vec{R}(\pi/a)$. The direction of $\Sigma\vec{R} := \vec{R}(0) + \vec{R}(\pi/a)$ may be interpreted as the polar axis of the electronic wave function. A nonzero $\Sigma\vec{R}$ connects different primitive unit cells and may be described as *intercellular*. The associated shift current is expected to be larger than in existing shift-current materials where intracellular charge transfer occurs between atoms in one unit cell.[18, 19]

Propositions (P1) and (P2) are topological principles to guide the search of materials with large shift currents. To quantify how large, I will use a figure of merit expressed in terms of the fundamental geometric quantity – the *shift connection*[6] $C_{mn}^{abb} = |A_{mn}^b|^2 R_{mn}^{ab}$. This quantity enters all expressions of the shift current [$j_s^a = \sigma_s^{abb}(\omega) E^b(\omega) E^a(-\omega)$] in various levels of approximation: nonlinear response,[7, 20, 21] semiclassical kinetic,[2, 22] Floquet,[22] Floquet-Keldysh[8]. One can view $[eE^b(\omega)][eE^a(-\omega)][eC_{mn}^{abb}]\delta(\hbar\omega - \epsilon_c + \epsilon_v)/\hbar$ as a transition rate of the electron-hole dipole moment, due to the monochromatic-optical excitation of an electron from the valence band (with energy ϵ_v) to the conduction band (ϵ_c). Mo-

tivated instead by a broadband light source (e.g., solar light) with an intensity shoulder that is as wide as a typical band, I integrate the rate over all optical excitations between the two bands lying closest to the Fermi level; the resultant quantity is proportional to the Brillouin-zone-integral of the shift connection:

$$F^{abb} = \int_{BZ} d^3k C_{mn}^{abb}, \quad \int \sigma_s^{abb} \Big|_{T=0} d\omega = d_s F^{abb} \frac{e^3}{h^2}. \quad (2)$$

I adopt F^{abb} as a dimensionless figure of merit. One exact interpretation of $d_s F^{abb} e^3/h^2$ ($d_s=2$ being the spin degeneracy) is as the frequency-integrated shift conductivity in the weak-field/strong-scattering regime,[8, 22] assuming independent particles with a zero-temperature distribution.²

For intrinsically polar insulators with a band gap E_g (minimized over the BZ), a band width E_w (maximized between conduction and valence band), a polar axis parallel to y , and a reflection symmetry mapping $x \rightarrow -x$, I propose that:

(Q1) For $E_g \gtrsim E_w$, $|F^{yxx}| \gg 1$ and is roughly proportional to the magnitude of the intercellular shift vector $\Sigma\vec{R}$.

Because $\Sigma\vec{R}$ is equivalently viewed as a \mathbb{Z}^2 -valued invariant taking values in a two-dimensional (2D) Bravais lattice with all lattice periods set to unity, proposition (Q1) epitomizes a maxim that to maximize the shift current is to maximize a topological invariant. (Q1) also challenges a widely-held expectation that small band gaps are necessary for large shift currents in topological materials.[11–13, 16, 24] Because being topologically nontrivial is a global property of the entire band, the largeness of $\sigma_s^{yxx}(\omega)$ extends over a frequency range comparable to the band width; this makes intrinsically polar insulators suited for solar cell applications, since the solar spectrum has a broad peak covering 2 to 3 eV. Solar cells based on the shift mechanism have comparative advantages to p-n junctions, including photovoltages which greatly exceed the band gap,[25, 26] and the potential to exceed the ‘detailed balance limit’[27] for the efficiency of solar power conversion.

(Q2) For $E_g \ll E_w$, F^{yxx} diverges as $|E_g|^{-1/2}$ in the approach to a topological phase transition.

This suggests an application to ultrafast infrared detection without an external bias voltage, which obviates the problem of the dark current in semimetallic photodetectors.[28]

To compare with known/predicted values for F^{abc} , Tan and Rappe have computed (by first principles) the longitudinal F^{aaa} for 950 noncentrosymmetric, nonmagnetic materials,[24] finding: (a) $|F^{yyy}| \approx 10^{-2}$ for the prototypical ferroelectric insulator BaTiO_3 , with y parallel to the polar

² Such a cold distribution is approximately valid in the sub-picosecond[19, 23] interval at the onset of radiation,[18] and is directly probed by ultrafast, THz-emission spectroscopy.[19, 23]

axis, and (b) $|F^{yyy}| \approx 3$ for SrAlSiH represents the best-performing insulator with $E_g \geq 1\text{eV}$; the former material has been experimentally benchmarked,[29, 30] but not the latter.

For a further comparison with typical values of $\sigma_s^{abb}(\omega)$, let us assume that an intrinsically polar insulator has a band width of $E_w = 1\text{eV}$ and that $\Sigma\vec{R}$ is proportional to a primitive Bravais lattice vector \vec{B} , with $||\vec{B}|| = b$. Proposition (Q1) then implies that the magnitude of the *frequency-averaged* shift conductivity $|\langle\sigma_s^{yxx}\rangle| \gtrsim [0.1\text{mAV}^{-2}] ||\Sigma\vec{R}||/b$, with $||\Sigma\vec{R}||/b$ an integer-valued topological multiplier. In contrast, the largest *peak* value $\sigma_s^{abb}(\omega)$ among five polar compounds $\{X\text{TiO}_3 (X=\text{Ba}, \text{Pb}), \text{LiAsS}_2, Y\text{AsSe}_2 (Y=\text{Li}, \text{Na})\}$ was calculated to be 0.05mAV^{-2} in magnitude.[29, 31]

Sec. II develops the general theory of intrinsically polar insulators to establish propositions (P1-2). Sec. III presents two model Hamiltonians of intrinsically polar insulators to corroborate propositions (Q1-2). The theory and models will first be established in the simplest possible context: a point group generated by a single reflection, a Bravais lattice with a monatomic basis, and a low-energy Hilbert space given by two bands. This context is expanded in Sec. IV; in particular, the extension to $(N > 2)$ bands leads naturally to identifying intrinsically polar insulators as having ‘delicate topology’.[32, 33] Throughout this work, I employ the tight-binding approximation for the Berry and shift connections, which is generally an uncontrolled approximation; Sec. V discusses how the approximation may be justified, as well as highlights an underappreciated pitfall. The last Section [Sec. VI] recapitulates our results with a different set of motivations, and further establishes the relevance of our results in a more complete theory of the bulk photovoltaic effect: inclusive of ballistic and excitonic currents. I end the paper by suggesting guidelines for an ab-initio-based, high-throughput search for noncentric insulators with nontrivial optical vorticity, and a different set of guidelines to search for intrinsically polar insulators.

II. THEORY OF INTRINSICALLY POLAR INSULATORS

Let us attempt to deduce the geometrical invariants of an intrinsically polar insulator from basic principles. One clue to determining the geometric quantity alluded to in proposition (P1) is that a nontrivial shift requires[1] breaking of spatial centrosymmetry. Let us therefore imagine what the geometry of band wave functions would look like, if these wave functions were to ‘maximally’ break centrosymmetry. Specifically, viewing the Berry curvature ($\Omega_v = \nabla \times \mathbf{A}_{vv}$) and the band-off-diagonal Berry connection as geometrical vector fields over momentum space, we will try to concoct fields that do the opposite of what centrosymmetry imposes.

A. Berry-curvature invariant that breaks centrosymmetry

Because the curvature transforms as a pseudovector under crystallographic point-group operations, $\Omega_v^z(k_x, k_y) = +\Omega_v^z(-k_x, -k_y)$ holds for any two-dimensional, centrosymmetric insulator; the theory will be extended to three dimensions later. To ‘maximally’ break centrosymmetry, let me (i) invert the sign in the centrosymmetry constraint to obtain: $\Omega_v^z(\mathbf{k}) = -\Omega_v^z(-\mathbf{k})$, and (ii) ask that the curvature integral [over *half* the Brillouin zone (BZ)] be quantized to a nontrivial integer:

$$RTP_v := \int_{BZ/2} \Omega_v^z \frac{d^2k}{2\pi} \in \mathbb{Z}. \quad (3)$$

The first condition is guaranteed by time-reversal symmetry; the sign difference in the symmetry constraints originates from time reversal having an antiunitary[34] representation \hat{T} squaring to the identity, in contrast with the unitary representation of spatial inversion.

The second condition [Eq. (3)] is possible if one introduces a reflection symmetry: $x \rightarrow -x$ and specifies $BZ/2$ to be the positive- k_x half of the BZ. (The integral of the curvature over the negative- k_x half of the BZ simply equals minus RTP_v due to time-reversal symmetry.) To specify the action of reflection symmetry, I consider a reduced Hilbert space given by the highest-energy valence band and the lowest-energy conduction band, and assume that this Hilbert space is spanned by two basis Wannier orbitals per primitive unit cell. (The restriction to two bands simplifies the initial presentation, but will be relaxed in Sec. IV.) Picking one representative unit cell, the two Wannier orbitals are labelled φ_e and φ_o , with the subscript indicating that one orbital is reflection-even and the other reflection-odd; I assume for now that both φ are centered at the same location, such that all the ‘Wannier centers’ form a rectangular lattice with a single-site basis and with periods a and b in the x and y directions respectively – this being a natural assumption if the two Wannier orbitals are atomic orbitals of the same atom. (The assumption of a single-site basis will also be relaxed in Sec. IV.) These assumptions on the Wannier orbitals translate to a symmetry constraint $\sigma_3 h(\mathbf{k}) \sigma_3 = h(-k_x, k_y)$ on the \mathbf{k} -periodic, two-by-two matrix Hamiltonian $h(\mathbf{k})$, with σ_3 the Pauli matrix representation of reflection. Eigenstates of $h(\mathbf{k})$ are denoted $|u_{mk}\rangle$ with corresponding energies ϵ_{mk} , with $m=v$ (resp. c) for the valence (resp. conduction) band, and $\epsilon_c > \epsilon_v$ for all \mathbf{k} .

Proof that RTP_v is integer-valued: Stoke’s theorem allows to equate $RTP_v = [Z_v(\pi/a) - Z_v(0)]/2\pi$, with $Z_n(k_x)$ the Berry-Zak phase acquired by parallel-transporting a Bloch state in band $n \in \{v, c\}$ over a \mathbf{k} -loop with fixed k_y :

$$Z_n(k_x) = \oint A_{nn}^y(k_x, k_y) dk_y, \quad (4)$$

with A_{nn} the intra-band Berry connection for the tight-binding eigenstate $|u_{nk}\rangle$. Denoting the parity (even vs odd) of a mirror-invariant Bloch state in band n by $p(n, k_x)$, it follows

from a known relation[3] between the Berry-Zak phase and the positional center of Wannier orbitals that

$$\text{for } k_x = 0 \text{ and } \frac{\pi}{a}, \quad \frac{Z_n(k_x)}{2\pi} =_1 \frac{y[\varphi_{p(n,k_x)}]}{b}, \quad (5)$$

with $=_1$ denoting an equality modulo one, and $y[\varphi_e]$ the y -positional center of the reflection-even basis Wannier orbital. The assumption of a single-site basis guarantees that $y[\varphi_{p(n,0)}] =_b y[\varphi_{p(n,\pi/a)}]$, implying that $Z_n(\pi/a) - Z_n(0)$ can only be an integer multiple of 2π , with this integer uniquely defined by insisting that the wave function is analytic over $BZ/2$. A representative, nontrivial example of the Berry-Zak phase is plotted in Fig. 1(a), with $Z_n(k_x)$ continuously increasing by 2π as k_x is advanced from 0 to π/a ; the reflection symmetry guarantees[35] that Z_n reverts to its original value upon further advancing k_x by π/a . Viewing k_x as an adiabatic parameter, $Z_n(k_x)$ represents the pumping of one quantum of charge over half an adiabatic cycle, and a reverse pump over the next half. This may be called a *reverting Thouless pump*, in contrast with the non-reverting pumps studied by Thouless.[36] (Reverting pumps have been previously studied in contexts unrelated to nonlinear optics.[32, 33, 37])

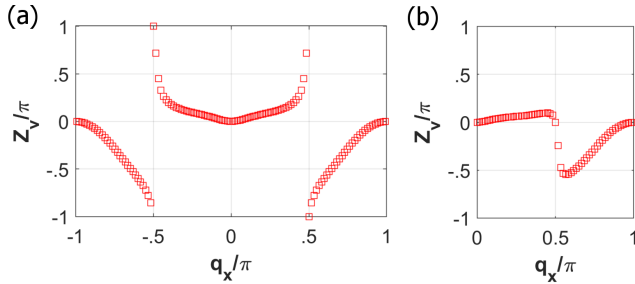


FIG. 1. (a) A reverting Thouless pump is revealed by a nontrivial dispersion of the valence-band Zak phase $Z_v(k_x)$ [Eq. (4)]; Z_v was computed with parameters $\alpha=2\beta=0.9$ in the model of Sec. III A. (b) A trivial pump for $\alpha=2\beta=1.1$.

B. Optical vortices break centrosymmetry

For the off-diagonal Berry connection field $A_{cv}^x(\mathbf{k})$, centrosymmetry is ‘maximally’ broken by introducing vortices, namely, quantized circulations of the phase field ϕ_{cv}^x around a \mathbf{k} -point where optical transitions vanish. For clarification, consider that $|A_{cv}^x|^2$ is proportional to the probability transition rate of resonant light absorption; I refer to $|A_{cv}^x|^2$ as the *optical affinity* between conduction and valence bands; \mathbf{k} -points where the affinity vanishes are called *optical zeros*. *Optical vortices* are optical zeros surrounded by a nontrivially circulating phase field.[38]

To visualize the circulation of the phase field, it is useful to introduce a Hamiltonian-vector interpretation of optical zeros and vortices: without loss of generality, I express $h(\mathbf{k}) = \mathbf{d}(\mathbf{k}) \cdot \boldsymbol{\sigma} + h_{id}(\mathbf{k}) I_{2 \times 2}$ as a dot product of a real three-vector \mathbf{d} (the *Hamiltonian vector*) with $\boldsymbol{\sigma} = (\sigma_1, \sigma_2, \sigma_3)$, plus

a term proportional to the two-by-two identity matrix. Applying the identity

$$A_{cv}^x = \langle u_c | \partial_{k_x} h | u_v \rangle / i(\epsilon_c - \epsilon_v), \quad (6)$$

one deduces that an optical zero (with a nonzero energy gap) exists if and only if $\mathbf{d} \times \partial_{k_x} \mathbf{d} = 0$. Since two real parameters (two spherical angles) need be tuned to align a vector \mathbf{d} to be collinear with $\partial_{k_x} \mathbf{d}$, optical zeros generically form $(d-2)$ -dimensional submanifolds of the d -dimensional BZ. For $d=2$, let us suppose an optical zero exists at the isolated wavevector \mathbf{k}_0 . For \mathbf{k} slightly deviating from \mathbf{k}_0 , \mathbf{d} and $\partial_{k_x} \mathbf{d}$ slightly deviate from being collinear. If \mathbf{k} is advanced in a small circle around \mathbf{k}_0 , the two vectors maintain their non-collinearity and are able to rotate relative to each other, like two partner dancers locked in the closed position.³ The relative rotation of $\partial_{k_x} \mathbf{d}$ around \mathbf{d} (as \mathbf{k} makes a full circle) defines an integer-valued rotation number that is equivalent to the winding number of the phase field ϕ_{cv}^x .

Because of the unitary-antiunitary distinction in the representations of spatial and temporal inversions, the former symmetry constrains $A_{cv}^x(\mathbf{k}) \propto A_{cv}^x(-\mathbf{k})$ (with a proportional phase factor that is analytic in \mathbf{k}), while the latter symmetry constrains $A_{cv}^x(\mathbf{k}) \propto \overline{A_{cv}^x(-\mathbf{k})}$ (with the accent denoting complex conjugation). It follows that centrosymmetry-related vortices have the same circulation while time-reversal-related vortices have the opposite. Thus, the presence of any optical vortex in a time-reversal-invariant Hamiltonian implies that centrosymmetry is broken.

C. Shift obstruction relation

Having identified two topological quantities that are fundamentally incompatible with centrosymmetry, I now relate their linear combination to an integral of the shift vector:

$$V - 2RT P_v = \Delta S = S(\pi/a) - S(0), \quad (7)$$

with V (the *net optical vorticity*) defined as the net circulation of all vortices of A_{cv}^x in $BZ/2$,⁴ and $S(k_x)$ defined as the *line-averaged shift* (in units of the lattice period b) of all quasiparticles with wavenumber k_x ,

$$\begin{aligned} S(k_x) &= \oint R_{cv}^{yx}(k_x, k_y) \frac{dk_y}{2\pi} \\ &= \frac{Z_c(k_x) - Z_v(k_x)}{2\pi} + \oint \partial_{k_y} \phi_{cv}^x \frac{dk_y}{2\pi}. \end{aligned} \quad (8)$$

³ https://en.wikipedia.org/wiki/Closed_position

⁴ The net vorticity is uniquely defined by $2\pi V = \int \partial_{k_y} \phi_{cv}^x(\pi/a, 0) dk_y - \int \partial_{k_y} \phi_{cv}^x(0, 0) dk_y$, with conduction-band and valence-band wave functions that are analytic over $BZ/2$. If one allows for the wave function to be defined over patches that cover $BZ/2$ and are mutually related by transition functions,[39] the net vorticity loses its unique definition.

ΔS is thus the difference in line-averaged shifts between the two mirror-invariant \mathbf{k} -lines. In deriving Eq. (7), I applied that time-reversal symmetry guarantees the existence of Bloch functions (for both bands) that are analytic and periodic functions of \mathbf{k} ,[40] hence A_{cv}^x is a meromorphic function of \mathbf{k} with discontinuities only at the optical vortices, and assumed in a generic situation that no vortices lie at a mirror-invariant wavevector; use was also made of the complementary relation between the curvatures of conduction and valence bands: $\Omega_v^z(\mathbf{k}) = -\Omega_c^z(\mathbf{k})$,[41] which leads to $RT P_v = -RT P_c$. Let me further remark on Eqs. (7)-(8):

(a) A closer inspection of Eq. (8) reveals that the line-averaged shift is integer-valued for mirror-invariant values of k_x . This follows from substitution of Eq. (5), with $y[\varphi_e] = y[\varphi_o]$ guaranteed by the lattice basis being monatomic. Combining this result with the symmetry constraint that $R_{cv}^{xx}(\mathbf{k})$ vanishes at all mirror-invariant wavevectors, we deduce that optically-excited quasiparticles with $k_x = 0$ are shifted by exactly $S(0)$ primitive lattice vectors parallel to the polar axis, on average. We thus arrive at proposition (P2), with the intercellular shift vectors: $\vec{R}(0) = S(0)b\vec{y}$ and $\vec{R}(\pi/a) = S(\pi/a)b\vec{y}$, and \vec{y} a unit vector in the y direction. (I will refer to the dimensionless scalars $S(0)$ and $S(\pi/a)$ as ‘intercellular shifts’, and ΔS as the ‘relative intercellular shift’.) It is worth emphasizing that the averaging process is essential for quantization, i.e., the shift vector at any specific \mathbf{k} is not quantized.

(b) Suppose $V - 2RT P_v$ in Eq. (7) is nonzero, and one has the ability to perturb the tight-binding Hamiltonian $h(\mathbf{k})$ and therefore modify $R_{cv}^{yx}(\mathbf{k})$. One would then encounter a *shift obstruction*: a topological obstruction against continuously tuning the shift vector to zero for all \mathbf{k} ; this is proposition (P1) in the introduction. (For this reason I refer to Eq. (7) as the *shift obstruction relation*.) But what exactly is meant by ‘continuously tuning’ in (P1)? In the traditional use of these words, continuity (with respect to \mathbf{k}) is imposed on the band-diagonal Berry connection of the valence band, and guaranteed by the standard assumption that the band gap $E_g(\mathbf{k})$ is nonzero. If a nonvanishing gap (throughout the BZ or some cross-section of it) is a sufficient condition for an invariant to be insensitive to symmetric Hamiltonian perturbations, such invariant (e.g., $RT P_v$) will be called a *standard invariant*. In optical phenomenon, we encounter non-standard invariants such as V whose definition assumes not only that the wave function is continuous over $BZ/2$ (as guaranteed by a nonzero band gap), but also that the band-off-diagonal Berry connection $A_{cv}^x(\mathbf{k}) = \langle u_c | i\partial_{k_x} u_v \rangle$ is continuous at all mirror-invariant \mathbf{k} . It is possible for A_{cv}^x to diverge when the band gap goes to zero, as is evident from the identity Eq. (6). Even if the band gap were everywhere nonzero, the existence of optical vortices would make A_{cv}^x vanishing and discontinuous. Both types of discontinuities are ruled out at a \mathbf{k} -point if both the energy gap and optical affinity are nonvanishing at that \mathbf{k} -point. This motivates a new definition: if the nonvanishing of the gap (in some BZ region) and the nonvanishing of the affinity (in a possibly distinct BZ region) are sufficient conditions for an invariant to be

insensitive to perturbations, such invariant (e.g., V , $S(0)$) that is not a standard invariant will be called an *optical invariant*. V relies on the gap being nonvanishing over $BZ/2$ and the affinity being nonvanishing for all mirror-invariant \mathbf{k} , while $S(0)$ relies on both gap and affinity being nonvanishing for wavevectors with $k_x = 0$.⁵ Because the shift obstruction relies on the insensitivity of the relative intercellular shift, the obstruction is also an optical invariant.

(c) A 2D reflection-symmetric insulator with $RT P_v = 0$ is deemed topologically trivial under every known classification scheme based on standard invariants: stable topology,[42–44] fragile topology,[45–48] delicate topology,[32, 33] topological quantum chemistry,[49] symmetry-based indicators,[50] and wilson-loop characterizations.[47, 48, 51, 52] What the shift obstruction relation reveals is that even such ‘trivial’ insulators can have a nontrivial optical vorticity, implying that at least one of the two intercellular shifts is nonzero. Conversely, being topologically nontrivial (in the standard sense) is not a sufficient condition for a shift obstruction, because it is possible for the optical-invariant contribution (V) to cancel out the standard-invariant contribution ($RT P_v$).

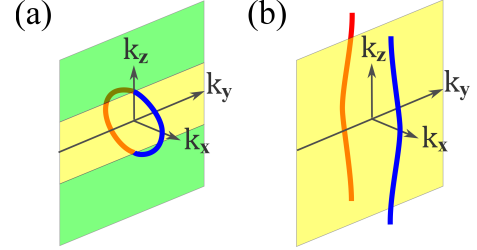


FIG. 2. (a) Intersection of a loop of optical zeros with the mirror-invariant \mathbf{k} -plane at $k_x = 0$. Red and blue distinguish between different segments of the optical-zero loop with opposite circulations. The net vorticity $V(k_z)$ is discontinuous at two values of k_z where the yellow plane meets either green plane. (b) Representative example of optical-zero loops that extend across a nontrivial cycle of the Brillouin torus.

(d) For three-dimensional, intrinsically polar insulators with mirror-invariant \mathbf{k} -planes, all optical invariants (V , ΔS) in the shift-obstruction relation are generally piecewise-continuous, integer-valued functions of a third wavenumber k_z . Discontinuities can occur at isolated values of k_z where a line of optical zeros intersects the mirror-invariant \mathbf{k} -plane, as illustrated in Fig. 2(a); the intersection point may be viewed as the merging of two optical vortices with opposite circulation, as distinguished by red and blue in Fig. 2(a). The k_z dependence of optical invariants can be ignored for the 3D insulating models explored in the next Section, which are all made from

⁵ This difference is because $S(0)$ is an integral of the shift vector which is gauge-invariant (hence uniquely-defined) at each \mathbf{k} ; on the other hand, V is an integral of $\partial_{k_y} \phi_{cv}^x$ which is not gauge-invariant at each \mathbf{k} ; to uniquely define V requires that both valence-band and conduction-band wave functions be analytic over $BZ/2$.

stacking 2D insulators in the z direction with weak inter-layer coupling; a representative example is illustrated in Fig. 2(b). For intrinsically polar (semi)metals, the standard invariant $RT P_v$ may also be a piecewise-continuous, integer-valued function of k_z .

(e) While all quantities in the shift obstruction relation [Eq. (7)] were derived to be integer-valued for intrinsically polar insulators, actually Eq. (7) holds for any two-band insulator – with the caveat that $RT P_v$ and ΔS generically deviate from integer values, thus precluding a shift obstruction.

D. Implications for the shift connection

What directly enters expressions for the shift current is the shift connection $C_{cv}^{yx}(\mathbf{k}) = |A_{cv}^x|^2 R_{cv}^{yx}$, whose value I now estimate for intrinsically polar insulators. An estimate is also presented for our figure of merit: the BZ-integrated shift connection [Eq. (2)].

(i) $E_g \gtrsim E_w$: If one is not close to a band-gap-closing, topological phase transition, the characteristic scale of variation for the optical affinity is the BZ period. I therefore estimate the BZ-averaged optical affinity as $\langle |A_{cv}^x|^2 \rangle \sim (a/2\pi)^2$ by dimensional analysis. (This estimate is not affected by the possible existence of optical zeros, which occupy a measure-zero subregion of the BZ.) Assuming the *average intercellular shift* $\langle S \rangle = [S(0) + S(\pi/a)]/2$ is nonzero and independent of k_z , the BZ-averaged shift vector is estimated as $\langle R^{yx} \rangle \sim \langle S \rangle b$. Then our figure of merit [cf. Eq. (2)] $F^{yx} \sim \int d^3k \langle |A_{cv}^x|^2 \rangle \langle R^{yx} \rangle = 2\pi \langle S \rangle a/c$, with c the lattice period in the z direction. This is a plausibility argument to support proposition (Q1), with the identification $\Sigma \vec{R} = 2\langle S \rangle b \hat{y}$. If $\langle S \rangle$ were to vanish but not the individual intercellular shifts, then $C_{cv}^{yx}(\mathbf{k}) \sim a^2 b S(0)/(2\pi)^2$ for $k_x \approx 0$. These estimates will be corroborated by model Hamiltonians in the next Section.

(ii) $E_g \ll E_w$: Close to a topological phase transition, the minimal band gap (E_g) over the BZ enters as a new scale in the problem. Most directly, it enters in the denominator of Eq. (6), leading to a divergence of the optical affinity for \mathbf{k} at the band-touching point; less directly, $\langle u_c | \partial_{k_x} h | u_v \rangle$ in the numerator of Eq. (6) may also depend implicitly on E_g . The net effect of the explicit and implicit dependences is that the optical affinity may diverge as $|E_g|^{-2+\alpha}$, with $\alpha \geq 0$. I distinguish between *first-class* phase transitions where the optical affinity diverges as $|E_g|^{-1}$ and *second-class* transitions where the affinity diverges as E_g^{-2} . Due to these divergences, F^{yx} may potentially also diverge and greatly exceed the estimates made for $E_g \gtrsim E_w$ in the previous paragraph; but this is not self-evident a priori, because of the potentially-nontrivial \mathbf{k} -dependence of the shift connection near the wavevector of closest inter-band contact. Two models will be presented in the next Section: one for which the phase transition is second-class but F^{yx} does not diverge (and instead displays a weaker kink-type non-analyticity), and a second model for which the phase transition is first class and F^{yx} diverges as $|E_g|^{-1/2}$.

III. MODEL HAMILTONIANS OF INTRINSICALLY POLAR INSULATORS

Beside corroborating propositions (P1-2, Q1-2), the models below are meant to illustrate the complementary roles of the Berry-Zak phase and the optical vorticity in determining the intercellular shifts, as well as to give intuition on the type of tight-binding hoppings that result in a shift obstruction. One potentially surprising finding is that nontrivial optical vorticity (with a trivial Berry-Zak phase) leads to a large frequency-integrated shift conductivity, despite the shift connection vanishing at the \mathbf{k} -position of the optical vortex. Special attention is focused on identifying non-analyticities of shift-related quantities at various types of topological phase transitions.

A. Model with second-class phase transition

1. Flatband limit with zero optical vorticity

To realize a simple 2D model Hamiltonian with a reverting Thouless pump, I begin with the standard parametrization of a real-valued, unit-norm three-vector by two spherical angles: $\mathbf{d} = [\sin(\theta) \cos(\phi), \sin(\theta) \sin(\phi), \cos(\theta)]$, then replace (θ, ϕ) by dimensionless wavenumbers $(q_x, q_y) := (k_x a, k_y b)$ and define the Hamiltonian $h(\mathbf{k}) = \mathbf{d}(\mathbf{k}) \cdot \boldsymbol{\sigma}$. Take special note of the replacement of $\theta \in [0, \pi]$ with $q_x \in [-\pi, \pi]$. The motivation for this strange construction of the Hamiltonian is now evident: $\mathbf{d}(\mathbf{k})$ covers the unit-norm sphere as \mathbf{k} is varied over $BZ/2$; this covering happens again (but with opposite orientation) over the other half of the BZ. Applying Berry's relation between the Berry curvature and the solid angle subtended by $\mathbf{d}(\mathbf{k})$, [53] I establish that $RT P_v = 1$. This can be alternatively established by computing the Zak phase as $Z_v = \pi[1 - \cos(q_x)]$.

By construction, the energy gap (separating flat conduction and valence bands) equals $2||\mathbf{d}(\mathbf{k})|| = 2$, which defines the energy scale for my dimensionless Hamiltonian. One may verify the forementioned reflection symmetry of the Hamiltonian, as well as a time-reversal constraint $\hat{T}h(\mathbf{k})\hat{T}^{-1} = h(-\mathbf{k})$ with $\hat{T} = \sigma_3 K$. The Fourier transform of $h(\mathbf{k})$ gives a real-space-dependent Hamiltonian with two intra-orbital hoppings over $(x, y) = (a, 0)$, and one inter-orbital hopping over (a, b) ; the presumed insignificance of hoppings parallel to the polar axis (y) requires that the Wannier orbitals are highly anisotropic. This requirement is in line with expectations that ideal shift-current materials necessarily have strongly delocalized and highly anisotropic covalent bonds. [24, 29] It is hoped that the simplicity of my model (having only three independent hoppings) offers a generalizable insight to the type of covalent bonding that is conducive to shift currents.

While flat bands are often associated to atomic insulators with a trivial shift connection, the flat bands in my model arise purely from the inter-site hopping matrix elements, and the

shift connection can be calculated as:

$$C_{cv}^{yxx}(\mathbf{k}) = -\frac{\epsilon_{\alpha\beta\delta}}{4} n_\alpha (\partial_{k_y} \partial_{k_x} n_\beta) (\partial_{k_x} n_\delta) = \left[\frac{a^2}{4} \right] \left[b \cos(q_x) \right],$$

with all indices on the Levi-Cevita tensor contracted with indices on $\mathbf{n} := \mathbf{d}/|\mathbf{d}|$. The \mathbf{n} -vector expression for the shift connection manifests its sole dependence on the wave function, i.e., the position on the Bloch sphere. The quantity in the first [resp. second] square bracket is identifiable with $|A_{cv}^x(\mathbf{k})|^2$ [resp. with $R_{cv}^{yx}(\mathbf{k})$]; it follows that there are no optical vortices ($V=0$) and the intercellular shifts are $S(0)=1=-S(\pi/a)$; the last equality, in combination with the previously-established $RT P_v=1$, establishes agreement with the shift obstruction relation. While the BZ-integral of C_{cv}^{yxx} vanishes, C_{cv}^{yxx} has a peak with maximum value $a^2 b S(0)/4$ at $k_x=0$, corroborating an estimate made in Sec. II. We see as a matter of principle that large values of the shift connection are attainable in the limit of an infinite band gap: $E_g/E_w=\infty$.

To induce a topological phase transition so that C_{cv}^{yxx} has a nonzero BZ-average, I introduce nearest and next-nearest inter-orbital hoppings in the x direction, which corresponds to the Hamiltonian perturbation: $\delta h(\mathbf{k}) = [\alpha \sin(q_x) + \beta \sin(2q_x)] \sigma_1$. The resultant phase diagram is shown in Fig. 3(a), with each phase labelled by four integer invariants: $\{V, RT P_v, S(0), S(\pi/a)\}$; the phase-transition lines are of two types that we subsequently deal with in turn.

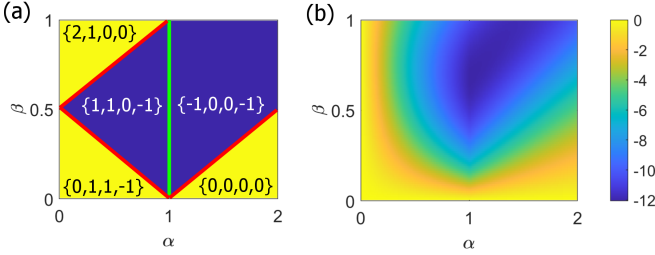


FIG. 3. (a) Phase diagram, with each phase is labelled by the invariants: $\{V, RT P_v, S(0), S(\pi/a)\}$. The yellow region indicates the average intercellular shift $\langle S \rangle = 0$; the dark blue region indicates $\langle S \rangle = -1/2$. (b) Figure of merit (F_{2D}^{yxx}) corresponding to the phase diagram, with the numerical value for F_{2D}^{yxx} indicated by a color bar.

2. Optical phase transition

The lines $\alpha+2\beta=1$, $\alpha-2\beta=1$ and $\alpha-2\beta=-1$ are colored red in Fig. 3(a), and mark *optical phase transitions* where the energy gap remains nonzero but the optical affinity vanishes at the reflection-invariant wavevector $(k_x, k_y) = (0, \pi)$, (π, π) and $(\pi, 0)$, respectively. Approaching a generic point on an optical transition line, a pair of reflection-related optical vortices (with opposite circulation) are either nucleated or annihilated, depending on the direction in which one approaches the transition point. To visualize this process, I employ the Hamiltonian-vector interpretation of optical vor-

trices [introduced near Eq. (6)] to track the \mathbf{k} -locations of optical zeroes and vortices – by plotting $|\mathbf{d} \times \partial_{k_x} \mathbf{d}|$ over the BZ. For instance, increasing $\alpha=2\beta=0$ from zero, the minimal optical affinity vanishes at the optical phase transition $\alpha=2\beta=1/2$ [Fig. 4(a)], and two optical vortices are nucleated for $\alpha=2\beta=5/8$ [Fig. 4(b)]. The single vortex in $BZ/2$ manifests also as a unit discontinuity in the k_x -dependent line-averaged shift, as illustrated in Fig. 4(c). On the other hand, the standard invariant $RT P_v$ is unchanged across an optical phase transition, because the energy gap does not vanish. The invariance of $RT P_v$ and the unit change in optical vorticity jointly imply that the relative intercellular shift must change by one unit, according to the shift obstruction relation [Eq. (7)].

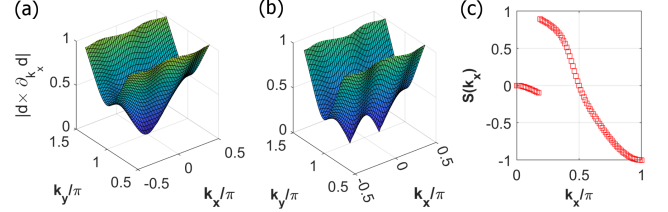


FIG. 4. (a-b) Zeroes of $|\mathbf{d} \times \partial_{k_x} \mathbf{d}|$ reveal optical zeroes, with \mathbf{d} the vector in the Hamiltonian $h(\mathbf{k}) = \mathbf{d}(\mathbf{k}) \cdot \boldsymbol{\sigma} + h_{id}(\mathbf{k}) I_{2 \times 2}$. The model parameters are $\alpha=2\beta=1/2$ and $5/8$, respectively, for panels (a) and (b). (c) The line-averaged shift $S(k_x)$ [Eq. (8)] for $\alpha=2\beta=5/8$. All lattice periods have been set to one.

3. Energetic phase transition

The $(\alpha=1)$ line is colored green in Fig. 3(a), and marks an *energetic phase transition* where the energy gap closes at only two non-symmetric wavevectors: $\mathbf{q} = (\pm\pi/2, \pi)$. For any point in the left half of the phase diagram ($\alpha < 1$), $RT P_v=1$ is deducible by energy-gap-preserving continuity to the flatband limit: $(\alpha, \beta) = (0, 0)$. Across the $\alpha=1$ line, the Zak phase $Z_v(\pi/2)$ changes discontinuously by π , resulting in $RT P_v=0$ for $\alpha > 1$.

To understand the π discontinuity, consider that the k_y -dependent Hamiltonian at fixed $q_x = \pi/2$ (and for any value of β) has a Hamiltonian vector with components: $d_1 = \cos q_y + \alpha$, $d_2 = \sin q_y$, $d_3 = 0$. Viewing (d_1, d_2) as a two-vector on a plane, the two-vector makes one full revolution around the origin as q_y is advanced by 2π , if $|\alpha| < 1$. Otherwise, no net revolution is made. This discontinuity in revolution number manifests as the Zak phase equalling π for $|\alpha| < 1$, and equalling zero otherwise. This discontinuous change in the Zak phase (at $q_x = \pi/2$) converts a reverting Thouless pump [illustrated in Fig. 1(a)] to a trivial pump [Fig. 1(b)].

A unit change in $RT P_v$ (that arises from a band touching at a non-symmetric wavevector) implies that the optical vorticity must change by two units, so as to satisfy the shift obstruction relation; this is because the relative intercellular shift is invariant across $\alpha=1$; recall that ΔS can only change if either

the energy gap or optical affinity vanishes at a mirror-invariant \mathbf{k} . How the optical vorticity changes by two (across $\alpha=1$) is a process of *vorticity inversion*: an optical vortex is ‘swallowed’ (at the band touching point) then ‘spat out’ with opposite circulation.

To understand this inversion, we return to the Hamiltonian-vector interpretation: recall that an optical vortex is an optical zero with nontrivial circulation, and an optical zero is a wavevector $\mathbf{k}_0(\alpha)$ where $\mathbf{d} \times \partial_{\mathbf{k}_x} \mathbf{d} = 0$. $\alpha=1$ marks a transition where \mathbf{d} and $\partial_{\mathbf{k}_x} \mathbf{d}$ change from being parallel to antiparallel; this is possible because $\mathbf{d}(\mathbf{k}_0(\alpha))$, being proportional to the energy gap, vanishes at the transition point. The inversion in the orientation of \mathbf{d} implies that, as \mathbf{k} is advanced in a small circle around \mathbf{k}_0 , the sense of relative rotation (between \mathbf{d} and $\partial_{\mathbf{k}_x} \mathbf{d}$) is also inverted – this is why the optical vortex flips its circulation.

4. Figure of merit

Over the same range for the Hamiltonian parameters (α, β) , Fig. 3(b) shows a numerically generated plot of the dimensionless figure of merit $F_{2D}^{yxx} := (2\pi/a) \int_{BZ} d^2k C_{cv}^{yxx}$, which is the 2D analog of F^{yxx} in Eq. (2). The numerical value for F_{2D}^{yxx} indicated by a color bar on the right of the figure panel. Comparison of panels (a) and (b) in Fig. 3 reveals:

(i) A positive correlation of F_{2D}^{yxx} with the average intercellular shift $\langle S \rangle$; the latter quantity vanishes in the yellow region of Fig. 3(a), and equals $-1/2$ in the dark blue region.

(ii) Phases with different $\langle S \rangle$ are separated by optical phase transitions [indicated by red lines in Fig. 3(a)]. Suppose one defines a trajectory on the phase diagram starting from $\langle S \rangle = 0$ (yellow region) and ending at $\langle S \rangle = -1/2$ (dark blue region), there is a continuous crossover in the value of F_{2D}^{yxx} from 0 to about -10 , if the trajectory does not start or end too close to an optical transition line. If the same trajectory does not intersect an energetic transition line (colored green), then the crossover (of F_{2D}^{yxx}) is not just continuous but smooth. One can verify the smoothness by asymptotic analysis: fixing $\alpha=2\beta$ and parametrizing the approach to the optical transition line ($\alpha+2\beta=1$) by a new variable $\delta=\alpha-1/2$; one finds that the shift vector diverges as $1/\delta$, but this divergence is cancelled by the vanishing of the optical affinity: $|A_{vc}^x|^2 \propto \delta^2$.

(iii) In contrast, there is a non-analyticity of F_{2D}^{yxx} across the energetic phase transition (green line, $\alpha=1$), because both the shift vector and the optical affinity diverge. For a quantitative analysis, let me introduce a new variable Q by $Q+1=\alpha=2\beta$. One finds that $|Q|$ is simply the minimal energy gap over the BZ, R_{cv}^{yx} diverges as $|Q|^{-1}$, and $|A_{vc}^x|^2$ diverges as Q^{-2} ; the latter observation implies that the phase transition is second-class, according to the classification made in Sec. II D. By dimensional analysis, one deduces that F_{2D}^{yxx} equals the sum of an analytic function of Q plus a non-analytic power series: $a_1/|Q| + a_2 \text{sgn}[Q] + a_3|Q| + \dots$. For this model, one can prove

$a_1=a_2=0$, which is partially understandable from the shift connection being odd under $(\delta k_x + Q/2) \rightarrow (-\delta k_x + Q/2)$ for sufficiently small $|Q|$ and $|\delta k_x|$; here, $\delta k_x = k_x - \pi/2$ is the wave number measured from the point of closest, inter-band contact. The leading term (in the power series) is then a kink-type non-analyticity, which is faintly visible in Fig. 3(a) as a darkening localized to the $(\alpha=1)$ -line, but is more evident in Fig. 5(a) where $F^{yxx}(\alpha, \beta)$ is shown as a three-dimensional surface plot.

(iv) Recall an earlier observation that $F_{2D}^{yxx} \approx -10$ in the trapezium-shaped phase on the right corner of Fig. 3(a). This phase represents an insulator with trivial Chern number and trivial reverting pump ($RT P_v = 0$); overall, this insulator would be considered trivial by the standard classification of topological insulators. The largeness of $|F_{2D}^{yxx}|$ is thus solely attributed to the nontrivial optical vorticity ($V=-1$). This attribution may surprise some readers, because the existence of an optical vortex implies that the optical affinity (hence also the shift connection) vanishes at the \mathbf{k} -position of the vortex. However such vanishing occurs only in a measure-zero \mathbf{k} -region with codimension two, i.e., only at isolated points in a 2D BZ. There is a competing and manifestly dominant factor: the vortex induces large variations of the shift vector over half the BZ period (according to the shift-obstruction relation), resulting in the average intercellular shift being $-1/2$ and $|F_{2D}^{yxx}| \gg 1$.

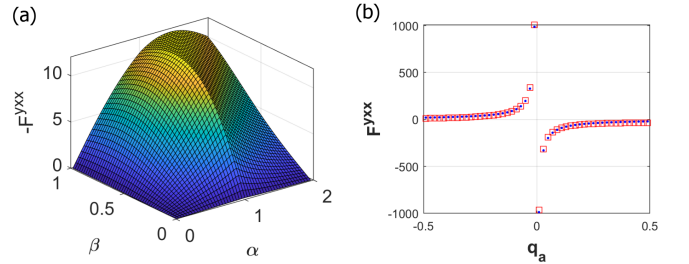


FIG. 5. (a) Kink-type non-analyticity of the figure of merit F_{2D}^{yxx} , for a second-class phase transition. (b) Divergent non-analyticity for a first-class phase transition modelled in Sec. III B: red squares represent a numerical integration, and blue dots represent an analytically-derived formula: $-\pi^2/q_a$.

One may view $h(\mathbf{k}) + \delta h(\mathbf{k})$ as a k_z -independent Hamiltonian for a 3D insulator that is constructed by stacking many layers of the 2D insulator with weak inter-layer coupling. Then the 2D figure of merit (of the 2D insulator) is simply proportional to the 3D figure of merit (of the 3D layered insulator): $F_{2D}^{yxx} = (a/c) F^{yxx}$, with a proportionality factor that is a ratio of lattice periods and is typically ≈ 1 . Then the observations made in (i-iv) above have 3D analogs which support proposition (Q1). In particular, $F^{yxx} \approx -10$ with $\langle S \rangle = -1/2$ is just slightly larger than an order-of-magnitude estimate ($F^{yxx} \sim 2\pi \langle S \rangle a/c$) made in Sec. II. However, because the leading non-analyticity of F^{yxx} is of the kink-type: $\sim |E_g|$, proposition (Q2) does not apply to the second-class phase transition of this model.

B. Model with first-class phase transition

To have F^{yxx} diverge as $|E_g|^{-1/2}$ [proposition (Q2)], I offer a different model Hamiltonian: $h(\mathbf{k}) = -(z^\dagger \sigma z) \cdot \sigma$ with

$$z(\mathbf{k}) = \begin{pmatrix} z_1 \\ z_2 \end{pmatrix} = \begin{pmatrix} \sin q_x \\ \sin q_y + i(q_a + \sum_{j=x,y} \cos q_j - 2) \end{pmatrix}. \quad (9)$$

$(q_x, q_y) = (k_x a, k_y b)$ are dimensionless wavenumbers, and q_a is a real-valued tuning parameter that induces the band gap ($=2z^\dagger z$) to close when $q_a=0, 2$ and 4; there are no optical transitions induced by q_a . I will focus on the $q_a=0$ transition where the band gap closes at $\mathbf{k}=(0, 0)$; an effective, low-energy Hamiltonian describing the transition is obtained by truncating the Taylor expansion of $z(\mathbf{k})$ with respect to \mathbf{k} :

$$h_t(\mathbf{k}) = -(z_t^\dagger \sigma z_t) \cdot \sigma, \quad z_t(\mathbf{k}) = \begin{pmatrix} q_x \\ q_y + i q_a \end{pmatrix}. \quad (10)$$

Reflection and time-reversal symmetries manifest as $\sigma_3 h(\mathbf{k}) \sigma_3 = h(-k_x, k_y)$ and $h(\mathbf{k}) = h(-\mathbf{k})$, respectively.

The form of the Hamiltonian is inspired by previous models of reverting Thouless pumps that are protected by a different crystallographic symmetry: rotation.[32, 33, 37] By design, $RT P_v$ changes by unity across $q_a=0$, which may be understood from a 2π -discontinuity of the Zak phase $Z_v(k_x=0)$ at a reflection-invariant \mathbf{k} -line. (This contrasts with the π -discontinuity of the Zak phase at a non-symmetric \mathbf{k} -line studied in the previous second-class phase transition.) A rough understanding of the 2π -discontinuity follows from inspecting the normalized, valence-band eigenvector solution to $h_t(\mathbf{k})$: $|u_v(\mathbf{k})\rangle = (-q_y + i q_a, q_x) / \sqrt{z_t^\dagger z_t}$, and realizing that the phase of $|u_v(0, k_y)\rangle$ changes by 2π as (q_y, q_a) is varied over a circle with radius $(q_y^2 + q_a^2)^{1/2}$.⁶ For $|q_a| \gg 1$, one deduces $RT P_v = 0$ from the simple form of the Hamiltonian $h(\mathbf{k}) \approx q_a^2 \sigma_3$; thus it must be that $RT P_v = -1$ for $q_a \in (0, 2)$.

What of the optical vortices? For large $|q_a|$, there are four vortices positioned at wavevectors $(q_x, q_y) \approx (\pm\pi/2, 0)$ and $(\pm\pi/2, \pi)$, with small corrections (of order $1/q_a$) to the q_x -component of these positions. The two vortices in $BZ/2$ have opposite circulation, hence the vorticity invariant V vanishes. As q_a approaches 0 from the negative side, two of the four vortices merge at the band-touching point and then mutually annihilate, leaving behind a net vorticity $V=1$ for

$q_a \in (0, 2)$.

Having determined $RT P_v$ and V , the shift obstruction relation tells us that the relative intercellular shift ΔS vanishes for $q_a < 0$ and equals $+1$ for $q_a \in (0, 2)$. Because of the integer-quantization of $S(0)$ and $S(\pi)$, the parities of ΔS and $S(0) + S(\pi) = 2\langle S \rangle$ must equal. A calculation gives explicitly that $\langle S \rangle = 0$ for $q_a < 0$ and $\langle S \rangle = -1/2$ for $q_a \in (0, 2)$. At the mid-point ($q_a=1$) between two energetic phase transitions, I numerically evaluate $F_{2D}^{yxx} = (a/2\pi) \int C_{cv}^{yxx} d^2 k \approx -39$, which is a factor of four larger than the analogous value for the previous model [Sec. III A 4].

The energetic phase transition is accompanied by the optical affinity diverging as q_a^{-2} , and the shift vector diverging as q_a^{-1} . Identifying $2z^\dagger z|_{\mathbf{k}=0} = 2q_a^2$ as the minimal band gap E_g , we deduce that the phase transition is first-class. From asymptotic analysis, $F_{2D}^{yxx} \approx c_1/q_a \approx c_1(2/E_g)^{1/2}$ for sufficiently small $|q_a|$, with c_1 a dimensionless constant. One can analytically evaluate $c_1 = -\pi^2/\sqrt{2}$, which is confirmed also by a numerical integration in Fig. 5(b).

Finally, if we view $h(\mathbf{k})$ as a k_z -independent Hamiltonian for a 3D insulator, then the divergence of the 2D figure of merit also applies to the 3D figure of merit: $F^{yxx} = (c/a) F_{2D}^{yxx}$, giving us proposition (Q2); one deduces also that $F^{yxx} \approx -39(c/a)$ for $\langle S \rangle \approx -1/2$, in support of proposition (Q1).

IV. GREATER VARIETY OF INTRINSICALLY POLAR INSULATORS

The main principles of intrinsically polar insulators have been formulated and exemplified in the simplest context, which however involves a few restrictive assumptions: (i) a Bravais lattice with a monatomic basis, (ii) a reduced Hilbert space of two bands, (iii) a point group generated by a single reflection. The first restriction is relaxed in Sec. IV A and the last two in Sec. IV B. It is hoped that a greater variety of intrinsically polar insulators increases the eventual probability of finding a material realization.

A. Beyond a monatomic basis

Thus far, I have assumed that the reduced Hilbert space is spanned by two Wannier orbitals per unit cell, and that the two orbitals in one representative unit cell are centered on the same location/site. (This restriction need not apply to Wannier orbitals outside the reduced Hilbert space.) Here we relax the spatial restriction and allow the two orbitals (in one representative cell) to be centered at different locations, subject to the constraints imposed by the space group.

Suppose the reflection-even orbital ϕ_e is centered at position \mathbf{w}_e , and ϕ_o at \mathbf{w}_o , then the tight-binding Hamiltonian becomes nonperiodic in translations by reciprocal lattice

⁶ For a more direct proof, consider that the valence-band eigenvector solution to $h(\mathbf{k})$ is $|u_v(\mathbf{k})\rangle = (-\bar{z}_2, z_1)/z^\dagger z$, which is practically unchanged as one tunes q_a across zero, except for $\sqrt{q_x^2 + q_y^2}$ small enough to be comparable to $|q_a|$. This implies that the 2π -discontinuity of the Zak phase $Z_v(0)$ [for $h(\mathbf{k})$] can be derived from a 2π -discontinuity of the continuum analog of the Zak phase: $Z_v^{ctm} = \int_{-\infty}^{\infty} A_{vv}^y(0, k_y) dk_y$, with the Berry connection A_{vv}^y a functional of the eigenvector solution of $h_t(\mathbf{k})$. This solution being simply $(-q_y + i q_a, q_x)/||\mathbf{q}||^2$, one deduces $Z_v^{ctm} = \pi \text{sgn}[q_a]$, as desired.

vector: $h(\mathbf{k}+\mathbf{G})=e^{-i\mathbf{G}\cdot\mathbf{w}}h(\mathbf{k})e^{i\mathbf{G}\cdot\mathbf{w}}$. \mathbf{w} here is a diagonal matrix with diagonal elements \mathbf{w}_e and \mathbf{w}_o . This nonperiodic relation is necessary[33] to maintain the mod-one equivalence between the tight-binding-approximated Berry-Zak phase and the Wannier center [cf. Eq. (5)], and justifies our interpretation of the tight-binding-approximated shift vector as a positional displacement.

Generically, the line-averaged shift [Eq. (8)] at a reflection-invariant value for k_x is no longer integer-valued: $S(0)=_1(y[\varphi_{p(c,0)}]-y[\varphi_{p(v,0)}])/b$. However, if the valence-band parities of both mirror-invariant \mathbf{k} -lines are identical: $p(v,0)=p(v,\pi/a)$, and likewise for the conduction band: $p(c,0)=p(c,\pi/a)\neq p(v,0)$, then the shift obstruction relation [Eq. (7)] holds, with $RT\mathcal{P}_v$ and ΔS remaining integer-valued; this follows from a simple generalization of the proof in Sec. II. The case of identical valence-band parities [$p(v,0)=p(v,\pi/a)$] is exemplified by the first-class model in Sec. III B, implying that the previous assumption of a monatomic basis is not needed for the quantization of ΔS .

It would seem for models with identical valence-band parities that proposition (P1) is preserved but (P2) lost. However, a statement exists for models (with or without identical parities) that is a close analog of (P2):

(P2') For intrinsically polar, 2D insulators with a reflection symmetry, a geometric quantity exists that inputs band wave functions over a reflection-invariant \mathbf{k} -line (say, $k_x=0$) and outputs an integer $\check{S}(0)$ with the following meaning: when a mirror-invariant quasiparticle (with $k_x=0$) is optically excited, it is displaced in the direction of the polar axis (y) with an averaged displacement $\check{S}(0)/b$ that is generically non-integer-valued. This displacement vector connects the center of a reflection-even Wannier orbital φ'_e with the center of a reflection-odd Wannier orbital φ'_o . In the standard tight-binding formalism, each Wannier orbital φ in the tight-binding Hilbert space is assigned to a primitive unit cell centered at a Bravais lattice vector ($n_x[\varphi]a, n_y[\varphi]b$), with n_x and $n_y\in\mathbb{Z}$. $\check{S}(0)=n_y[\varphi'_e]-n_y[\varphi'_o]$ if the conduction-band parity $p(c,0)$ is even; otherwise, $\check{S}(0)=n_y[\varphi'_o]-n_y[\varphi'_e]$.

I refer to $\check{S}(0)$ as the *generalized intercellular shift*. To define $\check{S}(0)$ in terms of the band wave function: suppose two representative orbitals φ_e and φ_o with respective positions \mathbf{w}_e and \mathbf{w}_o are assigned to the same cell, i.e., $n_j[\varphi_e]=n_j[\varphi_o]$ for $j=x$ and y . Then perform a unitary transformation on the \mathbf{k} -nonperiodic Hamiltonian so as to translate φ_o to lie 'atop' φ_e : $h(\mathbf{k})\rightarrow\tilde{h}(\mathbf{k})=U(\mathbf{k})^{-1}h(\mathbf{k})U(\mathbf{k})$, with $U(\mathbf{k})$ a diagonal matrix with diagonal elements 1 and $e^{i\mathbf{k}\cdot(\mathbf{w}_e-\mathbf{w}_o)}$. $\tilde{h}(\mathbf{k})$ is a \mathbf{k} -periodic Hamiltonian with the same band energies as $h(\mathbf{k})$, but with a modified wave function denoted by $|\tilde{u}_{ck}\rangle$ and $|\tilde{u}_{vk}\rangle$. Then $\check{S}(0)$ is defined exactly as $S(0)$ in Eq. (8), but with the functional dependence on u_{nk} replaced by a functional dependence

on \tilde{u}_{nk} .⁷ In the particular case that $\mathbf{w}_e=\mathbf{w}_o$, the unitary matrix is trivial, and the generalized intercellular shift reduces exactly to the previously-defined intercellular shift in Eq. (8).

B. Beyond two-band, reflection-symmetric Hamiltonians

For the purpose of counting, one band corresponds to a linearly-independent Bloch function over the BZ. For an ($N>2$)-band Hamiltonian with O conduction bands (indexed by c_1, \dots, c_O) and ($P=N-O$) valence bands (indexed by v_1, \dots, v_P), I define the *N -band intercellular shift* by summing over all inter-band intercellular shifts between the valence and conduction subspaces: $S_N(0)=\sum_{i=1}^O\sum_{j=1}^P\int R_{c_i v_j}^{yx}(0, k_y)dk_y/2\pi$. The utility of this definition is that if all Bloch states (in the conduction subspace, and with wavenumber $k_x=0$) are parity-even, and all Bloch states (in the valence subspace, and with $k_x=0$) are parity-odd, then the N -band intercellular shift remains quantized to integer values.⁸ (This statement holds as well if 'odd' is interchanged with 'even'.) If the just-mentioned parity condition applies also to Bloch states with $k_x=\pi/a$, then the N -band relative intercellular shift ($S_N(\pi/a)-S_N(0)$) is also quantized.

To recapitulate from a broader perspective, we began with a topological invariant that was previously defined for an M -band Hamiltonian, and were *conditionally* able to extend the meaning of this invariant to an ($N>M$)-band Hamiltonian. This condition specifies the allowable symmetry representations for all N bands in both conduction and valence subspaces. Conversely stated, the condition may be violated by adding a (topologically trivial) band with a disallowed symmetry representation to either conduction or

⁷ A generalized reverting Thouless pump invariant can also be similarly defined with u_{nk} in Eq. (3) replaced by \tilde{u}_{nk} . This generalization extends the meaning of a reverting pump beyond what has been considered in previous literature.[32, 33, 37] In the language developed in Ref. 33, the generalized pump exists assuming the 'mutually disjoint' symmetry condition, but not needing the 'iso-orbital' condition. A physical implication of the generalized pump is the existence of surface states that interpolate across the bulk gap, for an ideal (non-relaxed, non-reconstructed) surface termination that is compatible with the chosen unit cell.[33]

⁸ $2\pi S_N(0)=\sum_{i,j}\partial_{k_y}\phi_{c_i v_j}^x(0, k_y)dk_y+P\sum_i Z_{c_i}(0)-O\sum_j Z_{v_j}(0)$. The first of the three terms is a sum of phase winding numbers and therefore takes values in $2\pi\mathbb{Z}$. Under the just-stated assumption on the parities of the Bloch states, $\sum_{i=1}^O Z_{c_i}(0)/2\pi=1$ $\sum_{i=1}^O y[\varphi'_i]/b$, with $\{\varphi'_i\}_{i=1}^O$ labelling all reflection-even Wannier orbitals in a representative primitive unit cell. (If this identity is not apparent to the reader, I recommend Sec. VIII-C in Ref. 33 for a closely analogous proof with greater detail.) Likewise, $\sum_{j=1}^P Z_{v_j}(0)/2\pi=1$ $\sum_{j=1}^P y[\varphi'_j]/b$ for the reflection-odd Wannier orbitals in the same representative unit cell. For a monatomic basis of the Bravais lattice, $y[\varphi'_i]=y[\varphi'_j]$ for all i and j , hence $P\sum_i Z_{c_i}(0)-O\sum_j Z_{v_j}(0)$ vanishes modulo an integer multiple of 2π , completing the proof for $S_N(0)\in\mathbb{Z}$. If the assumption of a monatomic basis is relaxed, the generalized N -band intercellular shift $\check{S}_N(0)\in\mathbb{Z}$ has the meaning of the net change in the primitive unit cell label when all OP inter-band optical excitations are accounted for.

valence subspace. The consequence of violating the condition is that the N -band intercellular shift is no longer quantized to integer values. These, in a nutshell, are the hallmark attributes of *symmetry-protected delicate topology* – a notion that has been studied for standard invariants[32, 33] but is hereby extended to optical invariants.

Currently all known examples of delicate topological insulators are intrinsically noncentric,⁹ in the sense that the topological distinction between trivial and nontrivial insulators (in the standard sense) is only meaningful for space groups without centrosymmetry.[32, 33, 37, 55, 56] This offers a rich playing field to search for nontrivial optical invariants. To give a flavor of the possibilities, the reverting Thouless pump (RTP) has been theoretically explored in a wide variety of Pn -symmetric Hamiltonians,[32, 33, 37] where an n -fold rotational symmetry plays a role analogous to the reflection symmetry in this paper. A known mod- n equivalence[32, 33] between the RTP and Hopf invariants suggests the existence of mod- $2n$ shift obstruction relations that relate the intercellular shift, the Hopf invariant and the optical vorticity. In this context, the intercellular shift is defined by averaging the shift vector over rotation-invariant \mathbf{k} -lines, rather than a mirror-invariant cross-section of the BZ [cf. Eq. (8)].

V. THE TIGHT-BINDING APPROXIMATION OF THE SHIFT CURRENT: JUSTIFICATION AND PITFALLS

Having alluded to subtleties/dangers of the tight-binding approximation of shift quantities, I now elaborate on the nature of this approximation [Sec. V A], provide a semi-empirical [Sec. V B] and rigorous [Sec. V C] justification for the approximation, and finally highlight an under-appreciated pitfall of the approximation that is specific to two-band tight-binding models [Sec. V D].

A. Nature of the approximation

The shift connection is expressible in terms of the matrix elements of the non-Abelian Berry connection. In the rigorously accurate theory involving a Schrödinger-type Hamiltonian,[7] the Berry connection is defined by $\tilde{\mathbf{A}}_{ll'} = \langle \tilde{u}_{lk} | i \nabla_k \tilde{u}_{l'k} \rangle$, with $\tilde{u}_{lk}(\mathbf{r}) = \tilde{u}_{lk}(\mathbf{r} + \mathbf{R})$ the intracell component of the Bloch function that is periodic in lattice translations, and \mathbf{r} a *continuous* spatial coordinate within the primitive unit cell. However, throughout this work, I have approximated the Berry connection as $\mathbf{A}_{ll'} = \langle u_{lk} | i \nabla_k u_{l'k} \rangle$, with $u_{lk}(\alpha)$ the eigenvector of an N -band tight-binding Hamiltonian, and α a *discrete* intracell coordinate taking only N values. The error $\tilde{\mathbf{A}} - \mathbf{A}$ in the *discrete-space approximation* has an explicit expression [Eq.

(B8) in Ref. 51] in terms of matrix elements of the continuous-position operator in the basis of Wannier orbitals (there being N such orbitals per primitive unit cell); the approximation is equivalent to dropping all off-diagonal elements of the position operator in the just-mentioned Wannier basis – a point of view emphasized in Ref. 57. Because $\tilde{\mathbf{A}} - \mathbf{A}$ requires a correction, there is an analogous correction (derived explicitly in Ref. 57) to approximating the shift connection $\tilde{C}_{mn}^{abb} = |\tilde{A}_{mn}^b|^2 \tilde{R}_{mn}^{ab}$ by $C_{mn}^{abb} = |A_{mn}^b|^2 R_{mn}^{ab}$; here and henceforth, \tilde{O} is defined by $O[u_{lk}]$, for O that was previously defined as a functional of u_{lk} .

B. Semi-empirical justification of the approximation

The discrete-space approximation is generally uncontrolled, in the sense that no known small parameter exists to bound the error: $\delta C = \tilde{C}_{mn}^{abb} - C_{mn}^{abb}$. (A small parameter exists in specific cases, as elaborated in the next Sec. V C.) The next-best course of action is to compare δC to \tilde{C} in ab-initio-based studies where Wannier functions of a continuous spatial coordinate can be accurately obtained. These studies have been carried out for a number of materials;[57, 58] the most severe relative error [in the discrete-space approximation of $\tilde{\sigma}^{abb}(\omega)$] is reported as $\approx 50\%$ for BC_2N , and for frequencies close to a band-edge excitation;[58] the error is significantly milder over most other frequencies, and this holds for the other material case studies as well. A plausible conclusion from these studies is that it is safer for a tight-binding theorist to report a value of $\int \sigma^{abb} d\omega$ (integrated over a frequency range comparable to the bandwidth) rather than $\sigma^{abb}(\omega)$ at specific frequencies – this being another reason for my choice of the figure of merit F^{abb} in Eq. (2). This point of view is not universally adopted.[59]

C. Rigorous justification of the approximation

There is at least one place where δC is demonstrably negligible relative to \tilde{C} – in the proximity to a first-class phase transition in intrinsically polar insulators [Sec. III B]. More precisely, there exists a small parameter s (proportional to the square root of the minimal energy gap E_g) that allows to asymptotically compare δC and C ; one can prove that $\delta C/C \sim s$ as $s \rightarrow 0$. This implies not only that the asymptotic behavior $F^{yxx} \sim (E_g)^{-1/2}$ [proposition (Q2)] is preserved if δC is accounted for, but also that the coefficient c_1 in $F^{yxx} \approx c_1 (2/E_g)^{1/2}$ is unchanged by δC . The conclusion that δC is asymptotically irrelevant possibly generalizes to more classes of topological phase transitions, since the limit of vanishing energy gap is also the limit of long spatial wavelength, rendering short-wavelength variations [of $u_{lk}(\mathbf{r})$ within a unit cell] asymptotically irrelevant.

D. The discrete-space approximation for two bands

The discrete-space approximation of the shift conductivity is especially dangerous when used in conjunction with

⁹ Beyond insulators, there exists a phononic three-band touching point that is both delicate-topological and compatible with centrosymmetry.[54] It may be possible to generalize the homotopy invariant of this three-band touching to a centrosymmetric, three-band insulator.

two-band,¹⁰ time-reversal-invariant tight-binding models. Even if resonant excitations occur only between two bands, the shift connection generally receives contributions from virtual excitations to other intermediate bands, as has been made explicit by sum-over-states formulas in Ref. 21 and Ref. 59. Kraut and von Baltz have pointed out incontrovertibly that the *longitudinal shift conductivity* (σ^{aaa} with identical spatial indices) vanishes if one neglects all virtual excitations in the sum-over-state formula. That is to say, if one neglects any excitation to an intermediate band that is not either of the two bands of greater interest. This *Kraut-von Baltz selection rule* holds if $\langle \tilde{u}_m | \partial_{k_a} \partial_{k_b} H | \tilde{u}_n \rangle$ vanishes for $m \neq n$,^[59] with $H(\mathbf{k}) = e^{-i\mathbf{k} \cdot \mathbf{r}} \hat{H} e^{i\mathbf{k} \cdot \mathbf{r}}$ being the single-particle Bloch Hamiltonian; in particular, the rule holds if the Schrödinger-type Hamiltonian has the form $\hat{H} = p^2/2m + U(\mathbf{r}, \mathbf{p})$ with U that is at most linear in the canonical momentum \mathbf{p} ;¹¹ an example of such a linear term is the spin-orbit interaction.

Unfortunately, the selection rule has been underappreciated^[24] or mis-interpreted^[59] in recent works that purport to predict a value for σ^{aaa} (or upper limit for $\int \sigma^{aaa} d\omega$) based on two-band tight-binding models. In interpreting either of these works, one can take one of two positions:

(i) Suppose virtual excitations are exactly zero, then $\tilde{\sigma}^{aaa} = 0$, according to Kraut-von Baltz. Yet it is also possible for the two-band tight-binding approximation (σ^{aaa}) to be nonzero, due to $\langle u_c | \partial_{k_a}^2 h | u_v \rangle$ generically being nonzero in tight-binding models, as was correctly argued in Ref. 59. $\sigma^{aaa} = 0$ and $\tilde{\sigma}^{aaa} \neq 0$ are manifestly consistent statements, implying that the correction $\delta C = \tilde{C}_{mn}^{abb} - C_{mn}^{abb}$ (explicitly derived by Ibanez-Azpiroz-Tsirkin-Souza^[57]) exactly cancels C_{mn}^{abb} . This potentially surprising cancellation follows from adopting a pathological assumption.

(ii) Suppose virtual excitations to a third band are nonzero, then the Kraut-von Baltz selection rule does not hold. Then any two-band, tight-binding Hamiltonian cannot be a complete model of the longitudinal shift current, and any expression^[59] (or upper limit^[24]) for σ^{aaa} that depends only on parameters of a two-band, tight-binding Hamiltonian has questionable value.

It is worth remarking that even a minor absolute error in miscalculating the longitudinal shift connection is amplified to infinity in a calculation of the longitudinal shift conductivity,

if the joint density of states diverges – which unfortunately was the case in the band-edge calculations of Ref. 59.

Thus if a two-band tight-binding model is the preferred method, it is safer to predict the *transverse shift conductivity* $\int \sigma^{abb} d\omega$ (with $a \neq b$) rather than the longitudinal conductivity $\int \sigma^{aaa} d\omega$. This is one reason why only the transverse conductivity $\int \sigma^{yxx} d\omega$ (with y parallel to the polar axis) was explicitly calculated for the two-band models in Sec. III. The other reason is that it is only $\int \sigma^{yxx} d\omega$ that displays any extraordinary behavior for intrinsically polar insulators; in contrast, reflection symmetry imposes $\sigma^{xxx}(\omega) = \sigma^{xyy}(\omega) = 0$, and $C_{cv}^{yyy}(\mathbf{k})$ also vanishes at any reflection-invariant \mathbf{k} .

VI. DISCUSSION AND OUTLOOK

A. Recapitulation and fresh motivation of results

There has been a rich and fruitful tradition of identifying what properties a topological insulator absolutely cannot have, e.g., zero quantum entanglement,^[61–64] analytic Bloch functions,¹² symmetric Wannier functions which are localized to various degrees,^[32, 48, 49, 65–67] trivial Berry-Zak phase.^[47, 48, 51, 68, 69] This work demonstrates that intrinsically polar insulators are characterized by a *shift obstruction*: the inability to continuously tune the shift vector to zero throughout the Brillouin zone (BZ).

The shift obstruction exemplifies a new class of ‘optical invariants’ that depend on the off-diagonal Berry connection connecting valence and conduction bands.¹³ Consequently, the shift obstruction relies not just on the standard assumption of a nonvanishing energy gap, but also on a nonstandard assumption of a nonvanishing optical affinity. One implication is that the topological theory of nonlinear optical responses does not reduce or simplify to the standard theory of topological insulators. Topological insulators which are trivial in the standard classification can have nontrivial invariants in the ‘optotopological’ classification presented here. This classification is demonstrated in Sec. IV B to be an optotopological generalization of ‘symmetry-protected delicate topology’,^[32, 33] in the sense that the meaning of an optical invariant defined for a two-band Hamiltonian can be extended to an ($N > 2$)-band Hamiltonian, subject to conditions on the symmetry representations of all N bands.

A nontrivial shift obstruction generically implies a large frequency-integrated shift conductivity; this is supported by a plausibility argument [Sec. II] and model calculations [Sec. III]. Largeness has been quantified by a figure of merit

¹⁰ To clarify, time-reversal symmetry imposes that the minimal tight-binding model of an insulator has four bands, counting spin. I assume that the spin-orbit interaction is negligible and focus on one spin sector having only two bands. The Kraut-von Baltz selection rule (explained below) applies for negligible spin-orbit interaction.

¹¹ As was emphasized in Ref. 60, $\langle \tilde{u}_m | \partial_{k_a} \partial_{k_b} H | \tilde{u}_n \rangle$ might be nonzero for ab-initio calculations where the pseudopotential U may be nonlinear in \mathbf{p} . This is in principle one way to evade the selection rule, though further quantitative studies are needed to quantify this evasion.

¹² For related references, see Ref. 40 and footnote 12 in Ref. 65

¹³ My emphasis on topological aspects of the off-diagonal Berry connection is philosophically akin to a recent Riemannian-geometrical interpretation of the dipole matrix element^[6]

F^{abb} which is the BZ-integral of the shift connection [Eq. (2)].

It is worth elaborating on the physical significance of $|F^{abb}| \gg 1$. The theory of the shift current has been extended beyond nonlinear response[7, 20, 21] to describe non-equilibrium steady states subject to spontaneous[2] and stimulated[8, 22] radiative recombinations, as well as the formation of shallow excitons.[9] All these extensions have in common that the shift current is proportional to a BZ-integral of the shift connection weighted by a model- and \mathbf{k} -dependent factor; this factor could depend on the quasiparticle/photon distributions,[2] the dissipative strength,[8, 22] and the electron-hole interaction.[9] Assuming this \mathbf{k} -dependent factor does not lead to surprising cancellations (of the integrand) over the BZ, it is not implausible that $|F^{abb}| \gg 1$ is correlated with a large transverse shift current in all the extended theories.

A complete theory of the bulk photovoltaic effect should also account for the non-shift ('ballistic') current, which originates from an asymmetry of the quasiparticle distribution induced by intraband scattering.[70] This being wholly distinct from the interband shift mechanism, a large shift current does not necessarily imply a large ballistic current.¹⁴ In practice, a typical peak value for the frequency-dependent ballistic conductivity is $30 \mu A/V^2$ in magnitude,[71–73] which is small compared to the large shift conductivity we predict.

The topological perspective of the shift vector potentially has utility beyond the bulk photovoltaic effect. For instance, the shift vector also plays an important role in second harmonic generation,[8] and in ultrafast optical rectification for frequencies above the band gap.[18] The latter effect emits THz radiation that is desirable for spectroscopy.

B. Outlook for ab-initio-based material searches

1. Materials with nontrivial optical vorticity

To diagnose materials with large shift currents, other authors have proposed to compute the inter-band polarization difference, under the assumption that optical vortices are absent.[38] Such computation requires fixing the phase of the wave function over the entire BZ in the 'optical gauge',[38] which is a computationally expensive procedure. Moreover, if vortices were present, the interband polarization difference has questionable relevance to the shift current. It is therefore advantageous to directly relate the shift vector, the Berry-Zak phase and the optical vorticity on equal footing, without the ad hoc assumption that the vorticity vanishes. This relation is precisely given by the shift obstruction relation [Eq. (7)],

which shows that the net optical vorticity is a weighted sum of a difference in the Berry-Zak phase and a difference of the shift vector. For both quantities, the difference is between two high-symmetry regions of the BZ. (In contrast, the polarization is proportional to the *average* of the Berry-Zak phase over a reduced Brillouin zone.[4])

The shift obstruction relation [Eq. (7)] implies that optical vorticity can be helpful for shift-current materials. There are two competing effects of vorticity: while it is well-known that the shift connection vanishes *locally* at the \mathbf{k} -position of the vortex, vorticity also induces large variations of the shift vector over the scale of the BZ period (according to Eq. (7)), which plausibly implies the *momentum-integrated* shift connection is large. A model calculation in Sec. III A identifies the shift-vector variation as the dominating factor. Thus if one is interested in inducing a large bulk photovoltaic current by a *broadband* light source, even materials with trivial Berry-Zak phase and trivial polarization may be looked upon as favourable candidates – if they have nontrivial optical vorticity.

While the above argument for vorticity-induced shift variations has been verified for intrinsically polar insulators, actually the argument is sufficiently general to apply to insulators in any noncentric space group. The identification of nontrivial vorticity in a candidate noncentric material can be automated for a high-throughput ab-initio search. Here is one possible algorithm: (a) Identify pairs of 'optically-active' bands within an energy interval determined by the desired application (e.g., for solar-cell applications, the energy interval is determined by the solar spectrum); for each pair, ensure that one band lies in the valence subspace, and the other in the conduction subspace. (b) For each pair of optically-active bands labelled by c and v , compute the affinity $|A_{cv}^\alpha|^2$ on a \mathbf{k} -mesh over the Brillouin zone, for $\alpha = x, y, z$. The affinity is calculable from existing ab-initio techniques[29, 57, 60, 74] with at least one of these techniques being fully automated for high-throughput calculations.[74] (c) If for any \mathbf{k} on this mesh, the affinity lies below a pre-decided threshold, perform a gradient-descent algorithm to determine if the affinity is reducible to zero (within some reasonable tolerance). (d) If reducible, then compute the vorticity of the candidate optical zero by integrating $\nabla_{\mathbf{k}} \phi_{cv}^\alpha$ over a small \mathbf{k} -loop encircling the hypothesized \mathbf{k} -location of the optical zero, with ϕ_{cv}^α being the phase of A_{vc}^α .

2. Intrinsically polar materials

The ab-initio search for intrinsically polar insulators should be limited to polar space groups; the present theory predicts such insulators exist with the polar point groups C_s and C_n ($n=2, 3, 4, 6$), but future elaborations of the theory will likely expand this list. Insulators within this subset of space groups should be further filtered according to the symmetry representations of bands near the Fermi level [cf. Sec. IV B, as well as discussions of the 'mutually-disjoint' condition in Ref. 33]. For candidate materials that survive filtration, I propose to

¹⁴ A pathological counterexample may exist for band-edge optical excitations of ionic crystals with long-ranged electron-phonon interactions.[1] However, materials with large shift currents are likely to be highly covalent,[24, 29] which precludes ionic crystals.

compute the intercellular shift vector (or the generalized intercellular shift in Sec. IV A), which is an average of the shift vector R^{ab} over mirror- and/or rotation-invariant cross-sections of the BZ.¹⁵ (The shift vector is also calculable from existing ab-initio techniques.[29, 57, 60, 74]) For topologically nontrivial insulators, only the transverse intercellular shift is expected to be large, with a parallel to a polar axis and b orthogonal to any polar axis. A further calculation of the Berry-Zak phase[69, 75] will reveal whether a shift obstruction (if present) derives from a reverting Thouless pump or a nontrivial optical vorticity or a linear combination of both factors, in accordance with the shift obstruction relation in Eq. (7).

ACKNOWLEDGMENTS

My heartfelt gratitude goes to Chong Wang who acted graciously as my sounding board, and to Boris Sturman for patiently fielding endless questions on research he accomplished four decades ago. This work has benefitted from discussions with Takahiro Morimoto, Liang Tan, Joel Moore, Gao Lingyuan, Jay Sau, Ahn Junyeong, Joshua Deutsch, Penghao Zhu and Aleksandra Nelson.

-
- [1] B. I. Sturman and V. M. Fridkin, *The Photovoltaic and Photorefractive Effects in Noncentrosymmetric Materials* (Gordon and Breach Science Publishers, 1992).
- [2] B. S. V.I. Belinicher, E.L. Ivchenko, Kinetic theory of the displacement photovoltaic effect in piezoelectric, Soviet Physics JETP **56**, 359 (1982).
- [3] J. Zak, Berry's phase for energy bands in solids, Phys. Rev. Lett. **62**, 2747 (1989).
- [4] R. D. King-Smith and D. Vanderbilt, Theory of polarization of crystalline solids, Phys. Rev. B **47**, 1651 (1993).
- [5] R. Resta, Macroscopic polarization in crystalline dielectrics: the geometric phase approach, Rev. Mod. Phys. **66**, 899 (1994).
- [6] J. Ahn, G.-Y. Guo, N. Nagaosa, and A. Vishwanath, Riemannian geometry of resonant optical responses, Nature Physics **10**, 1038/s41567-021-01465-z (2021).
- [7] J. E. Sipe and A. I. Shkrebtii, Second-order optical response in semiconductors, Phys. Rev. B **61**, 5337 (2000).
- [8] T. Morimoto and N. Nagaosa, Topological nature of nonlinear optical effects in solids, Science Advances **2**, 10.1126/sciadv.1501524 (2016).
- [9] T. Morimoto and N. Nagaosa, Topological aspects of nonlinear excitonic processes in noncentrosymmetric crystals, Phys. Rev. B **94**, 035117 (2016).
- [10] F. de Juan, A. G. Grushin, T. Morimoto, and J. E. Moore, Quantized circular photogalvanic effect in weyl semimetals, Nature Communications **8**, 15995 (2017).
- [11] J. Ahn, G.-Y. Guo, and N. Nagaosa, Low-frequency divergence and quantum geometry of the bulk photovoltaic effect in topological semimetals, Phys. Rev. X **10**, 041041 (2020).
- [12] C.-K. Chan, N. H. Lindner, G. Refael, and P. A. Lee, Photocurrents in weyl semimetals, Phys. Rev. B **95**, 041104 (2017).
- [13] X. Yang, K. Burch, and Y. Ran, Divergent bulk photovoltaic effect in weyl semimetals (2018), arXiv:1712.09363 [cond-mat.mes-hall].
- [14] G. B. Osterhoudt, L. K. Diebel, M. J. Gray, X. Yang, J. Stanco, X. Huang, B. Shen, N. Ni, P. J. W. Moll, Y. Ran, and K. S. Burch, Colossal mid-infrared bulk photovoltaic effect in a type-i weyl semimetal, Nature Materials **18**, 471 (2019).
- [15] K. W. Kim, T. Morimoto, and N. Nagaosa, Shift charge and spin photocurrents in dirac surface states of topological insulator, Phys. Rev. B **95**, 035134 (2017).
- [16] L. Z. Tan and A. M. Rappe, Enhancement of the bulk photovoltaic effect in topological insulators, Phys. Rev. Lett. **116**, 237402 (2016).
- [17] N. W. Ashcroft and N. D. Mermin, *Solid state physics* (Thomson Learning, 20 Channel Center Street, Boston, MA 02210, USA, 1976).
- [18] F. Nastos and J. E. Sipe, Optical rectification and shift currents in gaas and gap response: Below and above the band gap, Phys. Rev. B **74**, 035201 (2006).
- [19] L. Braun, G. Mussler, A. Hruban, M. Konczykowski, T. Schumann, M. Wolf, M. Münzenberg, L. Perfetti, and T. Kampfrath, Ultrafast photocurrents at the surface of the three-dimensional topological insulator Bi_2Se_3 , Nature Communications **7**, 13259 (2016).
- [20] W. Kraut and R. von Baltz, Anomalous bulk photovoltaic effect in ferroelectrics: A quadratic response theory, Phys. Rev. B **19**, 1548 (1979).
- [21] R. von Baltz and W. Kraut, Theory of the bulk photovoltaic effect in pure crystals, Phys. Rev. B **23**, 5590 (1981).
- [22] T. Barik and J. D. Sau, Nonequilibrium nature of nonlinear optical response: Application to the bulk photovoltaic effect, Phys. Rev. B **101**, 045201 (2020).
- [23] M. Sotome, M. Nakamura, J. Fujioka, M. Ogino, Y. Kaneko, T. Morimoto, Y. Zhang, M. Kawasaki, N. Nagaosa, Y. Tokura, and N. Ogawa, Spectral dynamics of shift current in ferroelectric semiconductor SbSI , Proceedings of the National Academy of Sciences **116**, 1929 (2019), <https://www.pnas.org/content/116/6/1929.full.pdf>.
- [24] L. Z. Tan and A. M. Rappe, Upper limit on shift current generation in extended systems, Phys. Rev. B **100**, 085102 (2019).
- [25] P. Brody, Large polarization-dependent photovoltages in ceramic $\text{BaTiO}_3 + 5 \text{ wt percent } \text{CaTiO}_3$, Solid State Communications **12**, 673 (1973).
- [26] A. M. Glass, D. von der Linde, and T. J. Negran, High-voltage bulk photovoltaic effect and the photorefractive process in LiNbO_3 , Applied Physics Letters **25**, 233 (1974).
- [27] W. Shockley and H. J. Queisser, Detailed balance limit of efficiency of p-n junction solar cells, Journal of Applied Physics **32**, 510 (1961), <https://doi.org/10.1063/1.1736034>.
- [28] J. Liu, F. Xia, D. Xiao, F. J. García de Abajo, and D. Sun, Semimetals for high-performance photodetection, Nature Materials **19**, 830 (2020).

¹⁵ In contrast, the usual practice in the ab-initio community is to compute the \mathbf{k} -dependent shift connection over the BZ and integrate the connection to obtain either $\sigma_s^{abb}(\omega)$ or $\int \sigma_s^{abb} d\omega$. My proposal to compute the intercellular shift requires minimal modification of existing ab-initio packages, and merely redirects the spotlight to a different shift-related quantity defined over fewer \mathbf{k} -points.

- [29] S. M. Young and A. M. Rappe, First principles calculation of the shift current photovoltaic effect in ferroelectrics, *Phys. Rev. Lett.* **109**, 116601 (2012).
- [30] W. T. H. Koch, R. Munser, W. Ruppel, and P. Würfel, Anomalous photovoltage in batio₃, *Ferroelectrics* **13**, 305 (1976).
- [31] J. A. Brehm, S. M. Young, F. Zheng, and A. M. Rappe, First-principles calculation of the bulk photovoltaic effect in the polar compounds liass₂, liasse₂, and naasse₂, *The Journal of Chemical Physics* **141**, 204704 (2014).
- [32] A. Nelson, T. Neupert, T. c. v. Bzdušek, and A. Alexandradinata, Multicellularity of delicate topological insulators, *Phys. Rev. Lett.* **126**, 216404 (2021).
- [33] A. Nelson, T. Neupert, A. Alexandradinata, and T. Bzdušek, Delicate topology protected by rotation symmetry: Crystalline hopf insulators and beyond (2021), arXiv:2111.09365 [cond-mat.mes-hall].
- [34] E. Wigner, Ueber die operation der zeitumkehr in der quantenmechanik, *Nachrichten von der Gesellschaft der Wissenschaften zu Göttingen, Mathematisch-Physikalische Klasse*, 546 (1932).
- [35] A. Alexandradinata, Z. Wang, and B. A. Bernevig, Topological insulators from group cohomology, *Phys. Rev. X* **6**, 021008 (2016).
- [36] D. J. Thouless, Quantization of particle transport, *Phys. Rev. B* **27**, 6083 (1983).
- [37] A. Alexandradinata, A. Nelson, and A. A. Soluyanov, Teleportation of berry curvature on the surface of a hopf insulator, *Phys. Rev. B* **103**, 045107 (2021).
- [38] B. M. Fregoso, T. Morimoto, and J. E. Moore, Quantitative relationship between polarization differences and the zone-averaged shift photocurrent, *Phys. Rev. B* **96**, 075421 (2017).
- [39] B. A. B. with Taylor L. Hughes, *Topological Insulators and Topological Superconductors* (Princeton University Press, 2013).
- [40] G. Panati, Triviality of Bloch and Bloch–Dirac Bundles, *Ann. Henri Poincaré* **8**, 995 (2007).
- [41] A. Alexandradinata, C. Fang, M. J. Gilbert, and B. A. Bernevig, Spin-orbit-free topological insulators without time-reversal symmetry, *Phys. Rev. Lett.* **113**, 116403 (2014).
- [42] A. Kitaev, Periodic table for topological insulators and superconductors, *AIP Conf. Proc.* **1134**, 22 (2009).
- [43] K. Shiozaki, M. Sato, and K. Gomi, Topological crystalline materials: General formulation, module structure, and wallpaper groups, *Phys. Rev. B* **95**, 235425 (2017).
- [44] J. Kruthoff, J. de Boer, J. van Wezel, C. L. Kane, and R.-J. Slager, Topological classification of crystalline insulators through band structure combinatorics, *Phys. Rev. X* **7**, 041069 (2017).
- [45] H. C. Po, H. Watanabe, and A. Vishwanath, Fragile topology and wannier obstructions, *Phys. Rev. Lett.* **121**, 126402 (2018).
- [46] Z.-D. Song, L. Elcoro, Y.-F. Xu, N. Regnault, and B. A. Bernevig, Fragile phases as affine monoids: Classification and material examples, *Phys. Rev. X* **10**, 031001 (2020).
- [47] A. Bouhon, A. M. Black-Schaffer, and R.-J. Slager, Wilson loop approach to fragile topology of split elementary band representations and topological crystalline insulators with time-reversal symmetry, *Phys. Rev. B* **100**, 195135 (2019).
- [48] A. Alexandradinata, J. Höller, C. Wang, H. Cheng, and L. Lu, Crystallographic splitting theorem for band representations and fragile topological photonic crystals, arXiv e-prints, arXiv:1908.08541 (2019), arXiv:1908.08541 [cond-mat.str-el].
- [49] B. Bradlyn, L. Elcoro, J. Cano, M. G. Vergniory, Z. Wang, C. Felser, M. I. Aroyo, and B. A. Bernevig, Topological quantum chemistry, *Nature* **547**, 298 (2017), article.
- [50] H. C. Po, A. Vishwanath, and H. Watanabe, Symmetry-based indicators of band topology in the 230 space groups, *Nature Communications* **8**, 50 (2017).
- [51] A. Alexandradinata, X. Dai, and B. A. Bernevig, Wilson-loop characterization of inversion-symmetric topological insulators, *Phys. Rev. B* **89**, 155114 (2014).
- [52] B. Bradlyn, Z. Wang, J. Cano, and B. A. Bernevig, Disconnected elementary band representations, fragile topology, and wilson loops as topological indices: An example on the triangular lattice, *Phys. Rev. B* **99**, 045140 (2019).
- [53] M. V. Berry, Quantal phase factors accompanying adiabatic changes, *Proc. R. Soc. Lond A* **392**, 45 (1984).
- [54] S. Park, Y. Hwang, H. C. Choi, and B.-J. Yang, Topological acoustic triple point, *Nature Communications* **12**, 6781 (2021).
- [55] J. E. Moore, Y. Ran, and X.-G. Wen, Topological surface states in three-dimensional magnetic insulators, *Phys. Rev. Lett.* **101**, 186805 (2008).
- [56] B. Lapierre, T. Neupert, and L. Trifunovic, *n*-band hopf insulator, *Phys. Rev. Research* **3**, 033045 (2021).
- [57] J. Ibañez Azpiroz, S. S. Tsirkin, and I. Souza, Ab initio calculation of the shift photocurrent by wannier interpolation, *Phys. Rev. B* **97**, 245143 (2018).
- [58] J. Ibañez-Azpiroz, F. de Juan, and I. Souza, Assessing the role of interatomic position matrix elements in tight-binding calculations of optical properties, *SciPost Phys.* **12**, 70 (2022).
- [59] A. M. Cook, B. M. Fregoso, F. de Juan, S. Coh, and J. E. Moore, Design principles for shift current photovoltaics, *Nature Communications* **8**, 14176 (2017).
- [60] C. Wang, X. Liu, L. Kang, B.-L. Gu, Y. Xu, and W. Duan, First-principles calculation of nonlinear optical responses by wannier interpolation, *Phys. Rev. B* **96**, 115147 (2017).
- [61] A. M. Turner, Y. Zhang, and A. Vishwanath, Entanglement and inversion symmetry in topological insulators, *Phys. Rev. B* **82**, 241102 (2010).
- [62] T. L. Hughes, E. Prodan, and B. A. Bernevig, Inversion symmetric topological insulators, *Phys. Rev. B* **83**, 245132 (2011).
- [63] A. Alexandradinata, T. L. Hughes, and B. A. Bernevig, Trace index and spectral flow in the entanglement spectrum of topological insulators, *Phys. Rev. B* **84**, 195103 (2011).
- [64] Z. Huang and D. P. Arovas, Entanglement spectrum and wannier center flow of the hofstadter problem, *Phys. Rev. B* **86**, 245109 (2012).
- [65] A. Alexandradinata and J. Höller, No-go theorem for topological insulators and high-throughput identification of chern insulators, *Phys. Rev. B* **98**, 184305 (2018).
- [66] C. Brouder, G. Panati, M. Calandra, C. Mourougane, and N. Marzari, Exponential Localization of Wannier Functions in Insulators, *Phys. Rev. Lett.* **98**, 046402 (2007).
- [67] N. Read, Compactly supported wannier functions and algebraic *k*-theory, *Phys. Rev. B* **95**, 115309 (2017).
- [68] L. Fu and C. L. Kane, Time reversal polarization and a z [sub 2] adiabatic spin pump, *Phys. Rev. B* **74**, 195312 (2006).
- [69] R. Yu, X. L. Qi, A. Bernevig, Z. Fang, and X. Dai, Equivalent expression of \mathbb{Z}_2 topological invariant for band insulators using the non-abelian berry connection, *Phys. Rev. B* **84**, 075119 (2011).
- [70] V. I. Belinicher and B. I. Sturman, The photogalvanic effect in media lacking a center of symmetry, *Soviet Physics Uspekhi* **23**, 199 (1980).
- [71] B. I. Sturman, The photogalvanic effect in media lacking a center of symmetry, *Soviet Physics Uspekhi* **23**, 199 (2020).
- [72] A. V. L. et al., *Sov. Phys. Solid State* **30**, 1788 (1988).
- [73] Z. Dai, A. M. Schankler, L. Gao, L. Z. Tan, and A. M. Rappe, Phonon-assisted ballistic current from first-principles calcula-

- tions, Phys. Rev. Lett. **126**, 177403 (2021).
- [74] C. Wang, S. Zhao, X. Guo, X. Ren, B.-L. Gu, Y. Xu, and W. Duan, First-principles calculation of optical responses based on nonorthogonal localized orbitals, New Journal of Physics **21** (2019).
- [75] D. Gresch, G. Autès, O. V. Yazyev, M. Troyer, D. Vanderbilt, B. A. Bernevig, and A. A. Soluyanov, Z2pack: Numerical implementation of hybrid wannier centers for identifying topological materials, Phys. Rev. B **95**, 075146 (2017).